nature medicine

Megakaryocytes maintain homeostatic quiescence and promote post-injury regeneration of hematopoietic stem cells

Meng Zhao[1], John M Perry[1], Heather Marshall[1], Aparna Venkatraman[1,2], Pengxu Qian[1], Xi C He[1], Jasimuddin Ahamed[3] & Linheng Li[1,4]

Multiple bone marrow stromal cell types have been identified as hematopoietic stem cell (HSC)-regulating niche cells[1–7]. However, whether HSC progeny can serve directly as HSC niche cells has not previously been shown. Here we report a dichotomous role of megakaryocytes (MKs) in both maintaining HSC quiescence during homeostasis and promoting HSC regeneration after chemotherapeutic stress. We show that MKs are physically associated with HSCs in the bone marrow of mice and that MK ablation led to activation of quiescent HSCs and increased HSC proliferation. RNA sequencing (RNA-seq) analysis revealed that transforming growth factor β1 (encoded by *Tgfb1*) is expressed at higher levels in MKs as compared to other stromal niche cells. MK ablation led to reduced levels of biologically active TGF-β1 protein in the bone marrow and nuclear-localized phosphorylated SMAD2/3 (pSMAD2/3) in HSCs, suggesting that MKs maintain HSC quiescence through TGF-β–SMAD signaling[8,9]. Indeed, TGF-β1 injection into mice in which MKs had been ablated restored HSC quiescence, and conditional deletion of *Tgfb1* in MKs increased HSC activation and proliferation. These data demonstrate that TGF-β1 is a dominant signal emanating from MKs that maintains HSC quiescence. However, under conditions of chemotherapeutic challenge, MK ablation resulted in a severe defect in HSC expansion. In response to stress, fibroblast growth factor 1 (FGF1) signaling from MKs transiently dominates over TGF-β inhibitory signaling to stimulate HSC expansion[10,11]. Overall, these observations demonstrate that MKs serve as HSC-derived niche cells to dynamically regulate HSC function.

Although feedback from differentiated hematopoietic cells has been proposed as a mechanism to influence HSCs[12], genetic evidence for a role of HSC progeny cells in serving directly as HSC niche cells has not previously been shown. Although macrophages have been reported to influence HSCs, they do so through indirect regulation of stromal niche cells, including osteoblasts and Nestin$^+$ perivascular cells[13,14]. Furthermore, depletion of macrophages affects erythropoiesis but not other lineages in the bone marrow[15], ruling out the possibility that macrophages can constitute a direct HSC niche. Previous studies have also shown that MKs expand the N-cadherin$^+$ endosteal niche to facilitate engraftment of donor-derived HSCs in irradiated mice and that coculture of HSCs with MKs slightly increases HSC proliferation *in vitro*[16–18]. However, an *in vivo* function of MKs in directly regulating HSCs remains largely unknown. In this work, we used genetic models to investigate the role of MKs in HSC regulation during homeostasis and under stress.

To examine the anatomical relationship between MKs and endogenous HSCs in mouse bone marrow, we identified MKs by immunostaining with von Willebrand factor (vWF) and identified HSCs as lineage (Lin)$^-$CD41$^-$CD48$^-$CD150$^+$ cells in bone marrow sections. We observed that 20.8% of HSCs were in direct contact with MKs and 48.6% were within two cell diameters (**Fig. 1a**,**b**)[3,19,20]. This result suggests a potential regulatory relationship between HSCs and MKs. *Pf4* (encoding platelet factor 4)-*cre* has been shown to be expressed exclusively in the MK lineage[21], and we confirmed this finding by examining the *Pf4-cre*; *Rosa26-td-tomato* (*R26R^{tdT}*) reporter line[22] (**Supplementary Fig. 1**). To investigate the role of MKs in HSC maintenance, we generated a *Pf4-cre* induced *DTR* (encoding diphtheria toxin receptor) line (*Pf4-cre*; *iDTR*), in which MKs are rendered sensitive to diphtheria toxin (DT)[23]. We administered three intraperitoneal injections of DT (one injection every other day) to *Pf4-cre; iDTR* mice and analyzed them on the first day after the last injection (**Fig. 1c**). We observed efficient ablation of MKs in *Pf4-cre*$^+$; *iDTR* mice compared to *Pf4-cre*$^-$; *iDTR* control mice treated concurrently with DT, as revealed by immunostaining for vWF$^+$ MKs (**Fig. 1d**) and H&E staining (**Supplementary Fig. 2**) and further confirmed by MK colony-forming unit (CFU) assay (93.3% decrease) and platelet counts (79.8% decrease) (**Fig. 1d**). We also noticed that MKs quickly recovered by the third day after the last injection of DT (**Supplementary Fig. 2**).

We next examined whether MK ablation would affect HSCs *in vivo*. Five days after MK ablation, we observed an increase in the frequency and absolute numbers of short-term HSCs (ST-HSCs; CD34$^+$FLK2$^-$Lin$^-$SCA1$^+$c-KIT$^+$ (LSK); 3.2-fold) and multipotent progenitor cells (MPPs; CD34$^+$FLK2$^+$LSK; 2.3-fold) but no significant

[1]Stowers Institute for Medical Research, Kansas City, Missouri, USA. [2]Centre for Stem Cell Research, Christian Medical College, Vellore, India. [3]Laboratory of Blood and Vascular Biology, Rockefeller University, New York, New York, USA. [4]Department of Pathology and Laboratory Medicine, University of Kansas Medical Center, Kansas City, Kansas, USA. Correspondence should be addressed to L.L. (lil@stowers.org).

Received 27 May; accepted 2 September; published online 19 October 2014; doi:10.1038/nm.3706

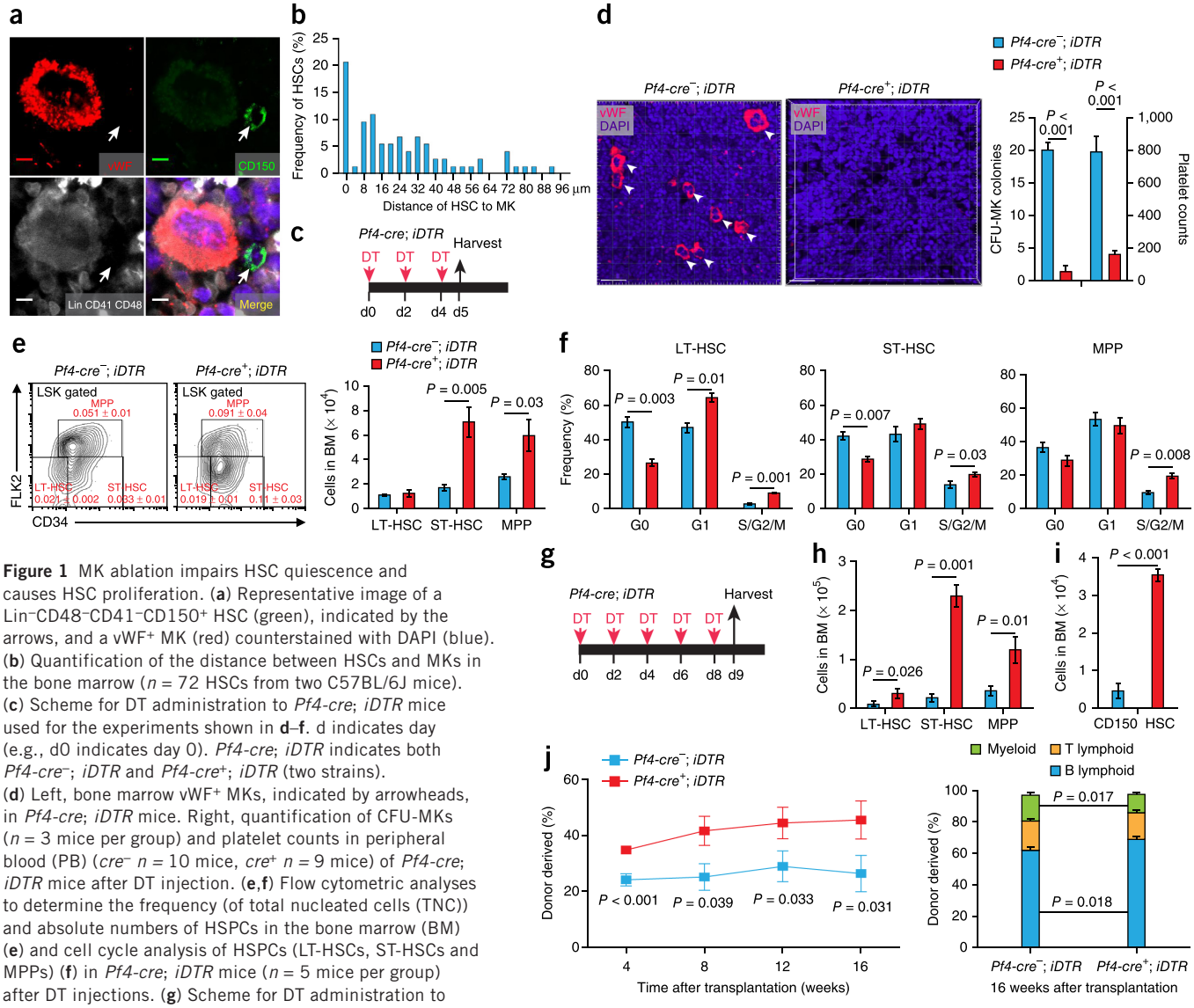

Figure 1 MK ablation impairs HSC quiescence and causes HSC proliferation. (**a**) Representative image of a Lin⁻CD48⁻CD41⁻CD150⁺ HSC (green), indicated by the arrows, and a vWF⁺ MK (red) counterstained with DAPI (blue). (**b**) Quantification of the distance between HSCs and MKs in the bone marrow ($n = 72$ HSCs from two C57BL/6J mice). (**c**) Scheme for DT administration to *Pf4-cre*; *iDTR* mice used for the experiments shown in **d**–**f**. d indicates day (e.g., d0 indicates day 0). *Pf4-cre*; *iDTR* indicates both *Pf4-cre*⁻; *iDTR* and *Pf4-cre*⁺; *iDTR* (two strains). (**d**) Left, bone marrow vWF⁺ MKs, indicated by arrowheads, in *Pf4-cre*; *iDTR* mice. Right, quantification of CFU-MKs ($n = 3$ mice per group) and platelet counts in peripheral blood (PB) (*cre*⁻ $n = 10$ mice, *cre*⁺ $n = 9$ mice) of *Pf4-cre*; *iDTR* mice after DT injection. (**e**,**f**) Flow cytometric analyses to determine the frequency (of total nucleated cells (TNC)) and absolute numbers of HSPCs in the bone marrow (BM) (**e**) and cell cycle analysis of HSPCs (LT-HSCs, ST-HSCs and MPPs) (**f**) in *Pf4-cre*; *iDTR* mice ($n = 5$ mice per group) after DT injections. (**g**) Scheme for DT administration to *Pf4-cre*; *iDTR* mice used for the experiments shown in **h**–**j**. (**h**,**i**) Absolute numbers of HSPCs in the bone marrow ($n = 4$ mice per group). CD150 HSC indicates CD150⁺CD48⁻LSK cells. (**j**) Quantification of functional HSCs by transplantation assay. PB analysis for total engrafted donor cells at the indicated number of weeks after transplantation and the percentage of donor-derived B, T and myeloid lineage cells at 16 weeks after transplantation ($n = 10$ mice per group). Error bars, s.e.m. Scale bars, 5 μm (**a**); 30 μm (**d**).

change in the frequency or absolute numbers of long-term HSCs (LT-HSCs; CD34⁻FLK2⁻LSK) (**Fig. 1e**)[24]. However, cell cycle analysis of LT-HSCs revealed a 1.9-fold decrease in the G0-phase fraction (from 50.3% to 26.4%) and concomitant increases in the G1-phase fraction (from 47.0% to 64.2%) and the G2/M-phase fraction (from 2.6% to 9.0%) in *Pf4-cre*⁺; *iDTR* mice compared to *Pf4-cre*⁻; *iDTR* controls (**Fig. 1f**). This finding, suggestive of activation of quiescent HSCs after MK depletion, led us to further examine HSC proliferation at a later time point after MK depletion. Indeed, 9 days after a series of five DT injections (**Fig. 1g**), *Pf4-cre*⁺; *iDTR* mice exhibited a significant increase in the populations of LT-HSCs (2-fold) and ST-HSCs (9.7-fold) (**Fig. 1h**). Notably, we also observed marked increases in the populations of CD150⁺CD48⁻LSK-marked HSCs (7.8-fold) (**Fig. 1i**) and CD150⁺CD105⁺LSK-marked HSCs[25] (15.3-fold) (**Supplementary Fig. 3**). We did not observe increased apoptotic or mobilized HSCs at either an early or late time point after MK depletion (**Supplementary Fig. 4**). These observations indicate that MK depletion leads to HSC activation and proliferation. Accordingly, bone marrow cells from *Pf4-cre*⁺; *iDTR* mice showed significantly higher levels of donor cell reconstitution (1.7-fold increase at 16 weeks) in irradiated mice compared to bone marrow cells from *Pf4-cre*⁻; *iDTR* controls treated concurrently with five injections of DT (**Fig. 1j**). We also observed that bone marrow cells from *Pf4-cre*⁺; *iDTR* mice were capable of multilineage reconstitution, although we observed an increased percentage of B lymphoid lineage cells (from 60% to 68.9%) and a decreased percentage of myeloid lineage cells (from 16.4% to 11.7%) (**Fig. 1j**). Overall, the effects of MK depletion suggest that MKs have a role in maintaining HSC quiescence by restricting their proliferation.

To search for potential molecular pathways involved in MK-mediated maintenance of HSC quiescence, we performed RNA-seq analysis in MKs and other stromal niche cell types. *Tgfb1* was more highly expressed than other known niche factors in MKs (**Fig. 2a** and **Supplementary Fig. 5**) and was more highly expressed in MKs than in other stromal niche cell types (Col2.3-GFP⁺ mature

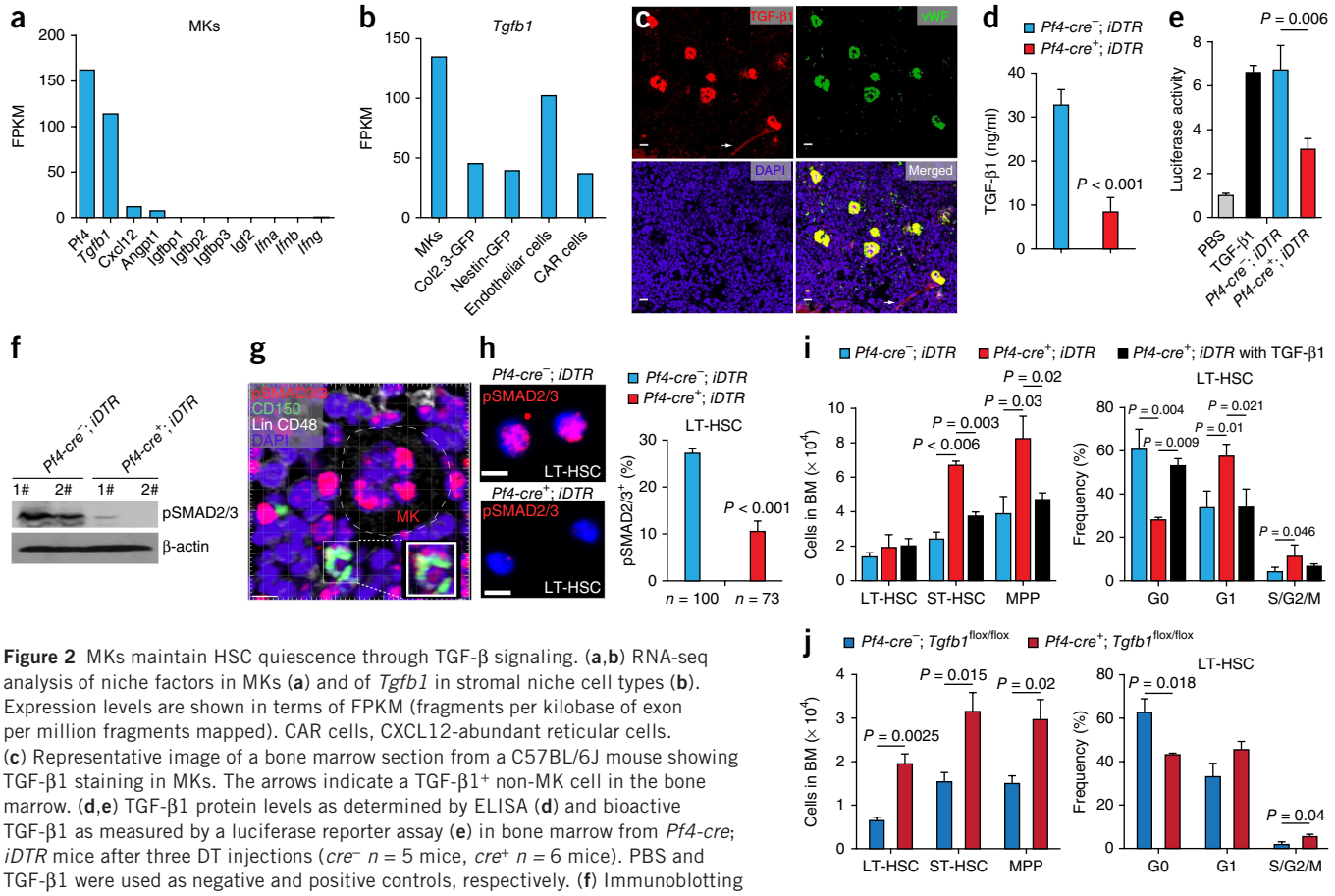

Figure 2 MKs maintain HSC quiescence through TGF-β signaling. (**a**,**b**) RNA-seq analysis of niche factors in MKs (**a**) and of *Tgfb1* in stromal niche cell types (**b**). Expression levels are shown in terms of FPKM (fragments per kilobase of exon per million fragments mapped). CAR cells, CXCL12-abundant reticular cells. (**c**) Representative image of a bone marrow section from a C57BL/6J mouse showing TGF-β1 staining in MKs. The arrows indicate a TGF-β1$^+$ non-MK cell in the bone marrow. (**d**,**e**) TGF-β1 protein levels as determined by ELISA (**d**) and bioactive TGF-β1 as measured by a luciferase reporter assay (**e**) in bone marrow from *Pf4-cre*; *iDTR* mice after three DT injections (*cre*$^-$ $n = 5$ mice, *cre*$^+$ $n = 6$ mice). PBS and TGF-β1 were used as negative and positive controls, respectively. (**f**) Immunoblotting for pSMAD2/3 protein in bone marrow cells. β-actin was used as a loading control. 1# and 2# indicate two individual mice. (**g**) Representative image of a bone marrow section from a C57BL/6J mouse showing an HSC with nuclear localization of pSMAD2/3 located adjacent to MKs. The dashed line outlines a MK, and the inset is magnified (1.5-fold) from the square box to the left. (**h**) Left, representative images of sorted LT-HSCs from *Pf4-cre*; *iDTR* mice immunostained with pSMAD2/3. Right, percentage of LT-HSCs from *Pf4-cre*; *iDTR* mice after DT injection that are pSMAD2/3 positive. (**i**,**j**) Absolute numbers, determined by flow cytometric analyses, and cell cycle analysis of HSPCs (LT-HSCs, ST-HSCs and MPPs) in *Pf4-cre*; *iDTR* mice after three injections of DT with or without TGF-β1 ($n = 4$ mice per group) (**i**) and in *Pf4-cre*; *Tgfb1*$^{flox/flox}$ mice (*cre*$^-$ $n = 4$ mice, *cre*$^+$ $n = 3$ mice) (**j**). Error bars, s.e.m. Scale bars, 20 μm (**c**); 5 μm (**g**,**h**).

osteoblasts, Nestin-GFP$^+$ perivascular cells, endothelial cells and chemokine (C-X-C motif) ligand 12 (CXCL12)-abundant reticular cells) (**Fig. 2b**), suggesting that MKs are the major source of TGF-β1 in the bone marrow. In immunostained bone marrow sections, TGF-β1 staining was present in MKs (**Fig. 2c**). In bone marrow from MK-depleted mice compared to control mice, TGF-β1 protein expression was reduced by 74.3% (**Fig. 2d**) by ELISA, and TGF-β1 biological activity was reduced by 54.7%, as assessed using a luciferase reporter assay (**Fig. 2e**). Activation of TGF-β downstream signaling, as revealed by pSMAD2/3 in bone marrow cells, was substantially reduced in MK-depleted animals (**Fig. 2f**).

Given the known function of TGF-β signaling in controlling HSC quiescence[8,9], we hypothesized that reduced TGF-β signaling caused by MK ablation might account for the observed activation of LT-HSCs. Indeed, we found that HSCs with nuclear-localized pSMAD2/3 were adjacent to MKs *in vivo* (**Fig. 2g**), and the number of pSMAD2/3$^+$ LT-HSCs was reduced 2.5-fold (from 27.2% to 10.5%) when MKs were depleted (**Fig. 2h**). To test whether MKs maintain HSC quiescence through TGF-β signaling, we injected recombinant TGF-β1 into MK-depleted mice. TGF-β1 injection prevented HSC activation and restored HSC quiescence (**Fig. 2i**), indicating that DT-induced MK ablation in *Pf4-cre*; *iDTR* mice results in loss of MK-derived TGF-β1 signaling, releasing HSCs from quiescence and increasing the proliferation of hematopoietic stem and progenitor cells (HSPCs).

We next took a genetic approach to conditionally delete *Tgfb1* in MKs using *Pf4-cre*$^+$; *Tgfb1*$^{flox/flox}$ mice. We observed that young *Pf4-cre*$^+$; *Tgfb1*$^{flox/flox}$ mice exhibited an overall increase in HSPC numbers (3.0-fold in LT-HSCs, 2.0-fold in ST-HSCs and 1.98-fold in MPPs) compared to *Pf4-cre*$^-$; *Tgfb1*$^{flox/flox}$ littermate controls (**Fig. 2j**). Cell cycle analysis showed that LT-HSCs from *Pf4-cre*$^+$; *Tgfb1*$^{flox/flox}$ mice exhibited a decreased G0-phase fraction (from 59% to 43.2%) and a concomitantly increased G1-phase fraction (from 36.4% to 45.6%) and G2/M-phase fraction (from 2.4% to 5.3%) (**Fig. 2j**). These data further support our conclusion that MKs maintain HSC quiescence primarily through TGF-β signaling. A complementary study (Bruns *et al.* in this issue[26]) shows that another major MK-secreted protein, PF4 (also called CXCL4), also negatively regulates HSC proliferation. This finding by Bruns *et al.*[26] also demonstrates the important role of MKs in maintaining HSC quiescence and suggests that MKs, similarly to other stromal niche cells, may produce a number of signals that regulate HSC function.

We next investigated whether MKs have a role in regulating HSC regeneration after chemotherapeutic injury. The cytotoxic agent 5-fluorouracil (5FU) initiates bone marrow stress by killing actively

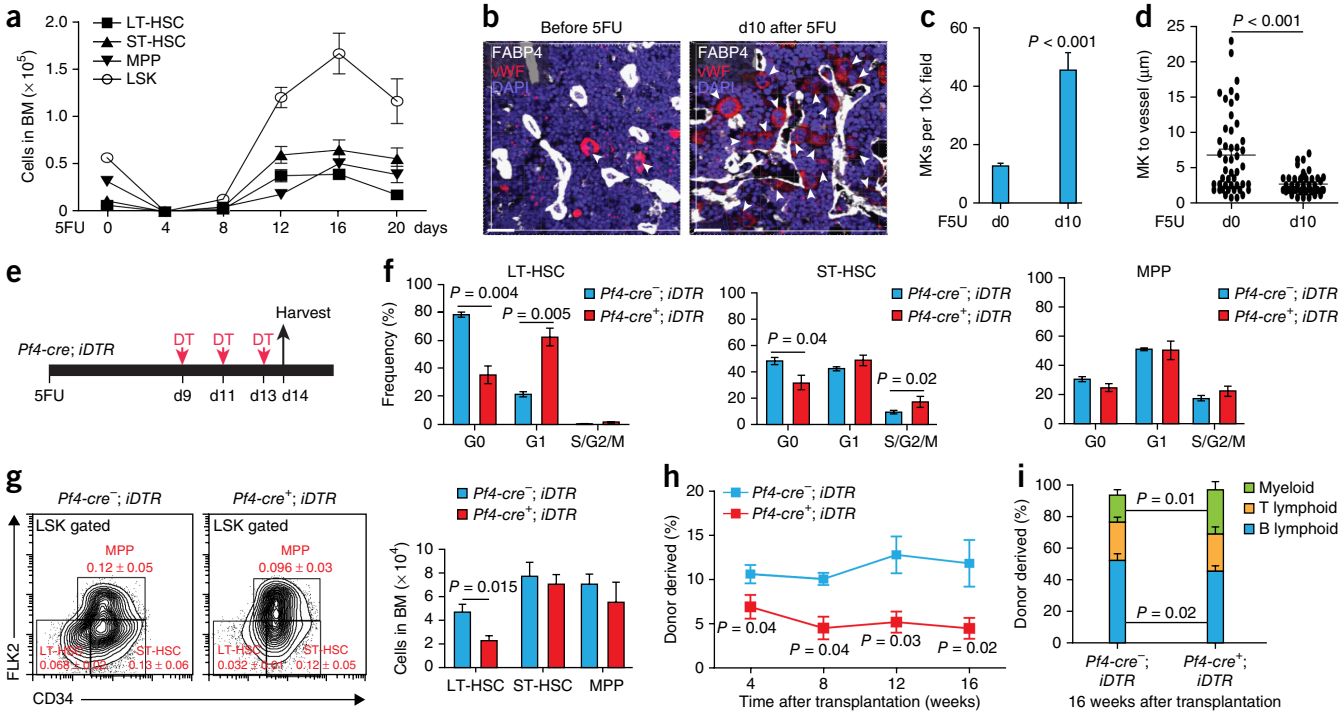

Figure 3 MK ablation causes an HSC regeneration defect after 5FU treatment. (**a**) HSPC (LSK, LT-HSC, ST-HSC and MPP) numbers in the bone marrow of C57BL/6J mice at the indicated times after 5FU treatment. (**b**) Representative image of bone marrow sections from C57BL/6J mice showing vWF$^+$ MKs (red), FABP4$^+$ blood vessels (white) and counterstaining with DAPI (blue). Arrowheads indicate MKs. (**c**,**d**) Quantification of the numbers of MKs per field of view in the bone marrow (**c**) and the distance of MKs to blood vessels in the bone marrow (**d**) in C57BL/6J WT mice at the indicated times after 5FU treatment ($n = 3$ mice per group). (**e**) Scheme for DT administration to *Pf4-cre*; *iDTR* mice after 5FU injection used for the experiments shown in **f**–**i**. (**f**,**g**) Cell cycle analysis of HSPCs (*cre*$^-$ $n = 6$, *cre*$^+$ $n = 4$) (**f**) and flow cytometric analyses (frequency in TNC) and absolute numbers of HSPCs in the bone marrow (*cre*$^-$ $n = 7$ mice, *cre*$^+$ $n = 5$ mice) (**g**) in *Pf4-cre*; *iDTR* mice after 5FU and DT injections. (**h**,**i**) Quantification of functional HSCs by transplantation assay. PB analysis for total engrafted donor cells at the indicated number of weeks after transplantation (**h**) and the percentage of donor-derived B, T and myeloid lineage cells at 16 weeks after transplantation (**i**) ($n = 10$ mice per group). Error bars, s.e.m. Scale bars, 30 μm (**b**).

cycling cells, including cycling HSCs[27], such that HSC numbers decline in the first week after 5FU treatment. Extensive cell death leads to activation of surviving quiescent HSCs, followed by sequential expansion of HSPCs from day 8 through day 16 after 5FU treatment to meet the increased hematopoietic demand[28], which we considered to be the critical period of HSC regeneration (**Fig. 3a**). At day 10 after 5FU treatment, we found that the number of MKs significantly increased (4.1-fold) and MKs migrated to blood vessels in the bone marrow (**Fig. 3b–d**)[29,30]. This observation indicates that MKs may have a role in regulating HSC regeneration after injury. To test this hypothesis, we depleted MKs during HSC regeneration by administering three DT injections from day 9 to day 13 after 5FU treatment and analyzed the consequences of this depletion at 14 days after 5FU treatment (**Fig. 3e**). Cell cycle analysis revealed that LT-HSCs from MK-ablated mice exhibited a 2.2-fold reduction in the G0-phase fraction (from 78.3% to 35.4%), with a concomitant 3-fold increase in the G1-phase fraction (from 21.3% to 62.4%) (**Fig. 3f**). Consistent with this observation, TGF-β1 protein expression in the bone marrow was reduced 85.7% in MK-depleted animals compared to controls (**Supplementary Fig. 6**). This finding is consistent with a prior report[31] that TGF-β1 restores HSC quiescence after chemotherapeutic stress. However, *Pf4-cre*$^+$; *iDTR* mice exhibited a severe defect in HSC expansion under chemotherapeutic stress. At 14 days after 5FU treatment, *Pf4-cre*$^+$; *iDTR* mice exhibited both a decreased frequency (52.1% decrease) and decreased absolute numbers (48.5% decrease) of LT-HSCs compared to *Pf4-cre*$^-$; *iDTR* controls (**Fig. 3g**). Consistent with this finding, bone marrow cells from *Pf4-cre*$^+$; *iDTR* mice showed significantly lower levels of donor cell reconstitution (56.1% decrease at 16 weeks) (**Fig. 3h**), with biased hematopoietic lineage reconstitution, compared to bone marrow cells from *Pf4-cre*$^-$; *iDTR* control mice (**Fig. 3i**). These findings raise the possibility that under chemotherapeutic stress conditions, the role of MKs switches to promote HSC expansion.

FGF signaling has been reported to be a transient signal for HSC expansion during HSC post-injury regeneration, and we have proposed previously that MKs produce FGFs during chemotherapeutic stress[10,11,32]. However, a role for MKs as a functionally important source of FGFs in supporting HSC regeneration has not been demonstrated. RNA-seq analysis revealed that *Fgf1* was the most highly expressed FGF ligand in bone marrow MKs (**Supplementary Fig. 7a**) and that MKs had the highest level of *Fgf1* expression compared to other stromal niche cell types (**Fig. 4a**), suggesting that MKs are the major source of FGF1 in the bone marrow. Consistent with a role for FGF1 in supporting HSC recovery after stress, FGF1 levels were increased sixfold in the bone marrow at 10 days after 5FU treatment in *Pf4-cre*$^-$; *iDTR* control mice (**Fig. 4b**), which correlated with an increase in the number of MKs in the bone marrow (**Fig. 3c**). Moreover, *Pf4-cre*$^+$; *iDTR* mice exhibited a 65.1% decline of FGF1 protein levels in the bone marrow at 10 days after 5FU treatment compared to *Pf4-cre*$^-$; *iDTR* mice (**Fig. 4b**). In contrast, there was a slight increase in FGF2 protein levels in MK-depleted mice (**Supplementary Fig. 7b**), presumably because of compensation from other cell types after MK ablation[11].

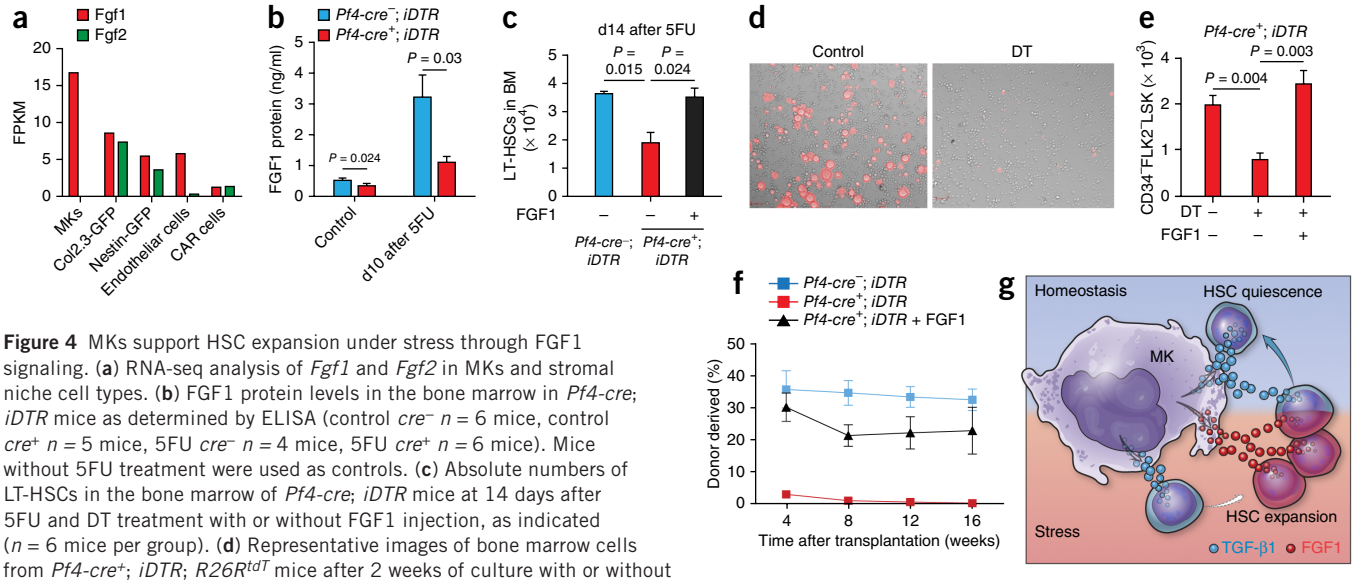

Figure 4 MKs support HSC expansion under stress through FGF1 signaling. (**a**) RNA-seq analysis of *Fgf1* and *Fgf2* in MKs and stromal niche cell types. (**b**) FGF1 protein levels in the bone marrow in *Pf4-cre*; *iDTR* mice as determined by ELISA (control *cre*$^-$ $n = 6$ mice, control *cre*$^+$ $n = 5$ mice, 5FU *cre*$^-$ $n = 4$ mice, 5FU *cre*$^+$ $n = 6$ mice). Mice without 5FU treatment were used as controls. (**c**) Absolute numbers of LT-HSCs in the bone marrow of *Pf4-cre*; *iDTR* mice at 14 days after 5FU and DT treatment with or without FGF1 injection, as indicated ($n = 6$ mice per group). (**d**) Representative images of bone marrow cells from *Pf4-cre*$^+$; *iDTR*; *R26R*^{tdT} mice after 2 weeks of culture with or without DT treatment. *Pf4-cre*–traced lineage cells (MKs and platelets) are shown as td-tomato–positive cells. (**e**) Absolute numbers of CD34$^-$FLK2$^-$LSK cells from the bone marrow of *Pf4-cre*$^+$; *iDTR* mice after addition of DT and FGF1 to the culture medium, as indicated, for 2 weeks ($n = 4$ per group). (**f**) Quantification of functional HSCs by transplantation assay. PB analysis for total engrafted donor cells at the indicated number of weeks after transplantation ($n = 5$ mice per group). Error bars, s.e.m. (**g**) Schematic showing the dynamic regulatory role of the MK niche. The MK niche maintains HSC quiescence through TGF-β signaling under homeostatic conditions; however, when rapid expansion of HSCs is required (under stressed conditions), FGF1 production by MKs promotes HSC expansion. Scale bars, 50 μm (**d**).

We next conditionally deleted *Fgfr1* in MKs. We observed that *Pf4-cre*$^+$; *Fgfr1*$^{flox/flox}$ mice had reduced MK expansion (65.6% decrease), decreased FGF1 (47.3% decrease) and reduced HSC regeneration (55.6% decrease of LT-HSC numbers and 45.9% decrease of donor cell reconstitution) in bone marrow compared to *Pf4-cre*$^-$; *Fgfr1*$^{flox/flox}$ mice at 14 days after 5FU treatment (**Supplementary Fig. 8**). These results indicate that MKs themselves depend on FGF signaling to expand their numbers, produce FGF1 and support HSC regeneration after injury. We propose that in response to chemotherapeutic stress, FGF1 levels are raised rapidly in the bone marrow by MKs in a positive feedback manner and, thus, FGF1 signaling from MKs transiently dominates over TGF-β inhibitory signaling, resulting in HSC expansion. Indeed, FGF1 injection restored LT-HSC numbers in MK-depleted mice at 14 days after 5FU treatment (**Fig. 4c**). Thus, although MK depletion under 5FU stress causes HSC activation (due to loss of TGF-β inhibitory signaling), loss of FGF1 signaling markedly suppresses HSC expansion, which ultimately results in a reduction of HSC numbers in the bone marrow.

We further investigated the role of MKs in an HSC *ex vivo* culture system, in which HSCs undergo an expansion that is similar to *in vivo* HSC regeneration after injury[33,34]. We adapted the culture system so that HSCs are cultured in the presence of only stem cell factor (SCF) and thrombopoietin (THPO), without other growth factors such as FGF. In this system, more MKs were produced than were cells of other lineages (**Supplementary Fig. 9**). This result led us to hypothesize that MKs might be functionally important for *ex vivo* expansion of HSCs. In support of this hypothesis, coculture of HSCs with MKs, but not with Lin$^+$ cells, significantly improved HSC engraftment (1.97-fold increase at 16 weeks, $P = 0.003$) (**Supplementary Fig. 10**), consistent with a previous report that MKs promote HSC proliferation *in vitro*[18]. Although it has been reported that *Pf4-cre* is expressed in long-term repopulating HSCs[35], *Pf4-cre*–traced bone marrow cells were not capable of reconstituting irradiated mice (**Supplementary Fig. 10a**).

We next examined the consequence of MK ablation in HSC *ex vivo* culture. As expected, DT treatment efficiently ablated the MK lineage in the culture system (**Fig. 4d**). After 2 weeks of culture with DT treatment, bone marrow cells from *Pf4-cre*$^+$; *iDTR* mice exhibited a 60.3% decline of CD34$^-$FLK2$^-$LSK cells (**Fig. 4e**); however, DT-treated control bone marrow cells from *Pf4-cre*$^-$; *iDTR* mice expanded normally (**Supplementary Fig. 11**). Furthermore, the reduction in HSC numbers in cultures of DT-treated bone marrow cells from *Pf4-cre*$^+$; *iDTR* mice was rescued completely by inclusion of FGF1 in the culture medium (**Fig. 4e**). To examine the number of functional HSCs after *ex vivo* expansion, we conducted a competitive repopulation assay and found that DT-treated cultures from *Pf4-cre*$^+$; *iDTR* mice lost significant engraftment capability compared to those from *Pf4-cre*$^-$; *iDTR* mice ($P < 0.001$) and that FGF1 robustly rescued this defect (70% recovery) (**Fig. 4f**). This result is consistent with our findings in the *in vivo* chemotherapy stress model, in that under conditions of both *in vivo* and *ex vivo* stress, FGF1 secreted from MKs promotes HSC expansion. Although inclusion of FGF1 in the culture medium led to full recovery of HSC numbers (**Fig. 4e**), engraftment capability was not fully replenished (**Fig. 4f**), suggesting that TGF-β signaling, which promotes quiescence, may be required for long-term HSC functional maintenance during HSC expansion *ex vivo*.

Here we show that MKs, a derivative of HSCs, function as niche cells to directly regulate HSCs. The MK niche dynamically changes its role between homeostatic and stress conditions: under homeostatic conditions, the MK niche maintains HSC quiescence through TGF-β signaling; however, when rapid expansion of HSCs is required, FGF1 production by MKs promotes HSC expansion (**Fig. 4g**). Moreover, this study opens a potential avenue for the clinical use of MKs in HSC expansion and recovery after chemotherapy and transplantation.

METHODS

Methods and any associated references are available in the online version of the paper.

Note: Any Supplementary Information and Source Data files are available in the online version of the paper.

ACKNOWLEDGMENTS

We are grateful to members of the Li lab for scientific discussion and manuscript critical reading, M. Hembree, K. Zapien, D. Dukes and B. Lewis for technical support and K. Tannen for manuscript editing and proofreading. We thank H. Lin (Massachusetts General Hospital), who generously provided the CAGA-luc plasmid. We thank C. Deng (US National Institutes of Health) for providing *Fgfr1*$^{flox/flox}$ mice. This work was funded by the Stowers Institute for Medical Research.

AUTHOR CONTRIBUTIONS

M.Z. performed experiments, analyzed data and wrote the paper. J.M.P. contributed to HSC culture studies and edited the manuscript. H.M. contributed to part of the mouse work. A.V., P.Q. and X.C.H. performed RNA-seq. J.A. shared reagents. L.L. directed the overall project and co-wrote the manuscript. All authors discussed the results and commented on the manuscript.

COMPETING FINANCIAL INTERESTS

The authors declare no competing financial interests.

1. Zhang, J. *et al.* Identification of the haematopoietic stem cell niche and control of the niche size. *Nature* **425**, 836–841 (2003).
2. Calvi, L.M. *et al.* Osteoblastic cells regulate the haematopoietic stem cell niche. *Nature* **425**, 841–846 (2003).
3. Kiel, M.J., Yilmaz, O.H., Iwashita, T., Terhorst, C. & Morrison, S.J. SLAM family receptors distinguish hematopoietic stem and progenitor cells and reveal endothelial niches for stem cells. *Cell* **121**, 1109–1121 (2005).
4. Sugiyama, T., Kohara, H., Noda, M. & Nagasawa, T. Maintenance of the hematopoietic stem cell pool by CXCL12-CXCR4 chemokine signaling in bone marrow stromal cell niches. *Immunity* **25**, 977–988 (2006).
5. Méndez-Ferrer, S. *et al.* Mesenchymal and haematopoietic stem cells form a unique bone marrow niche. *Nature* **466**, 829–834 (2010).
6. Ding, L., Saunders, T.L., Enikolopov, G. & Morrison, S.J. Endothelial and perivascular cells maintain haematopoietic stem cells. *Nature* **481**, 457–462 (2012).
7. Kunisaki, Y. *et al.* Arteriolar niches maintain haematopoietic stem cell quiescence. *Nature* **23**, 3865–3873 (2013).
8. Yamazaki, S. *et al.* TGF-β as a candidate bone marrow niche signal to induce hematopoietic stem cell hibernation. *Blood* **113**, 1250–1256 (2009).
9. Yamazaki, S. *et al.* Nonmyelinating Schwann cells maintain hematopoietic stem cell hibernation in the bone marrow niche. *Cell* **147**, 1146–1158 (2011).
10. Zhao, M. *et al.* FGF signaling facilitates postinjury recovery of mouse hematopoietic system. *Blood* **120**, 1831–1842 (2012).
11. Itkin, T. *et al.* FGF-2 expands murine hematopoietic stem and progenitor cells via proliferation of stromal cells, c-Kit activation, and CXCL12 down-regulation. *Blood* **120**, 1843–1855 (2012).
12. Li, L. & Clevers, H. Coexistence of quiescent and active adult stem cells in mammals. *Science* **327**, 542–545 (2010).
13. Winkler, I.G. *et al.* Bone marrow macrophages maintain hematopoietic stem cell (HSC) niches and their depletion mobilizes HSCs. *Blood* **116**, 4815–4828 (2010).
14. Chow, A. *et al.* Bone marrow CD169^{+} macrophages promote the retention of hematopoietic stem and progenitor cells in the mesenchymal stem cell niche. *J. Exp. Med.* **208**, 261–271 (2011).
15. Chow, A. *et al.* CD169^{+} macrophages provide a niche promoting erythropoiesis under homeostasis and stress. *Nat. Med.* **19**, 429–436 (2013).
16. Dominici, M. *et al.* Restoration and reversible expansion of the osteoblastic hematopoietic stem cell niche after marrow radioablation. *Blood* **114**, 2333–2343 (2009).
17. Olson, T.S. *et al.* Megakaryocytes promote murine osteoblastic HSC niche expansion and stem cell engraftment after radioablative conditioning. *Blood* **121**, 5238–5249 (2013).
18. Heazlewood, S.Y. *et al.* Megakaryocytes co-localise with hemopoietic stem cells and release cytokines that up-regulate stem cell proliferation. *Stem Cell Res.* **11**, 782–792 (2013).
19. Deutsch, V.R. & Tomer, A. Megakaryocyte development and platelet production. *Br. J. Haematol.* **134**, 453–466 (2006).
20. Xie, Y. *et al.* Detection of functional haematopoietic stem cell niche using real-time imaging. *Nature* **457**, 97–101 (2009).
21. Tiedt, R., Schomber, T., Hao-Shen, H. & Skoda, R.C. Pf4-Cre transgenic mice allow the generation of lineage-restricted gene knockouts for studying megakaryocyte and platelet function *in vivo*. *Blood* **109**, 1503–1506 (2007).
22. Madisen, L. *et al.* A robust and high-throughput Cre reporting and characterization system for the whole mouse brain. *Nat. Neurosci.* **13**, 133–140 (2010).
23. Buch, T. *et al.* A Cre-inducible diphtheria toxin receptor mediates cell lineage ablation after toxin administration. *Nat. Methods* **2**, 419–426 (2005).
24. Yang, L. *et al.* Identification of Lin^{-}Sca1^{+}kit^{+}CD34^{+}Flt3^{-} short-term hematopoietic stem cells capable of rapidly reconstituting and rescuing myeloablated transplant recipients. *Blood* **105**, 2717–2723 (2005).
25. Chen, C.Z. *et al.* Identification of endoglin as a functional marker that defines long-term repopulating hematopoietic stem cells. *Proc. Natl. Acad. Sci. USA* **99**, 15468–15473 (2002).
26. Bruns, I. *et al.* Megakaryocytes regulate hematopoietic stem cell quiescence through Cxcl4 secretion. *Nat. Med.* doi:10.1038/nm.3707 (19 October 2014).
27. Longley, D.B., Harkin, D.P. & Johnston, P.G. 5-fluorouracil: mechanisms of action and clinical strategies. *Nat. Rev. Cancer* **3**, 330–338 (2003).
28. Essers, M.A. *et al.* IFNα activates dormant haematopoietic stem cells *in vivo*. *Nature* **458**, 904–908 (2009).
29. Elmasri, H. *et al.* Fatty acid binding protein 4 is a target of VEGF and a regulator of cell proliferation in endothelial cells. *FASEB J.* **23**, 3865–3873 (2009).
30. Avecilla, S.T. *et al.* Chemokine-mediated interaction of hematopoietic progenitors with the bone marrow vascular niche is required for thrombopoiesis. *Nat. Med.* **10**, 64–71 (2004).
31. Brenet, F., Kermani, P., Spektor, R., Rafii, S. & Scandura, J.M. TGFβ restores hematopoietic homeostasis after myelosuppressive chemotherapy. *J. Exp. Med.* **210**, 623–639 (2013).
32. de Haan, G. *et al.* *In vitro* generation of long-term repopulating hematopoietic stem cells by fibroblast growth factor-1. *Dev. Cell* **4**, 241–251 (2003).
33. Zhang, C.C. *et al.* Angiopoietin-like proteins stimulate *ex vivo* expansion of hematopoietic stem cells. *Nat. Med.* **12**, 240–245 (2006).
34. Perry, J.M. *et al.* Cooperation between both Wnt/β-catenin and PTEN/PI3K/Akt signaling promotes primitive hematopoietic stem cell self-renewal and expansion. *Genes Dev.* **25**, 1928–1942 (2011).
35. Calaminus, S.D. *et al.* Lineage tracing of Pf4-Cre marks hematopoietic stem cells and their progeny. *PLoS ONE* **7**, e51361 (2012).

ONLINE METHODS

Animals. C57BL/6-Tg(*Pf4-cre*)Q3Rsko/J (*Pf4-cre*), C57BL/6-Gt(ROSA)26Sortm1(HBEGF)Awai/J (*iDTR*), B6.Cg-Gt(ROSA)26Sortm14(CAG-tdTomato)Hze/J (*R26R*^{tdT}) and *Tgfb1*tm2.1Doe/J (*Tgfb1*$^{flox/flox}$) mice were obtained from the Jackson Laboratory. *Fgfr1*$^{flox/flox}$ mice were kindly provided by C.-X. Deng (US National Institute of Diabetes and Digestive and Kidney Diseases, US National Institutes of Health). *Pf4-cre* mice were mated with the *iDTR* line to generate *Pf4-cre*; *iDTR* mice. To induce MK ablation in the *Pf4-cre*; *iDTR* model, DT (Sigma) was injected intraperitoneally every other day at a dose of 50 ng per g body weight into *Pf4-cre*; *iDTR* mice as indicated. *Tgfb1*$^{flox/flox}$ and *Fgfr1*$^{flox/flox}$ mice were mated with the *Pf4-cre* line to generate *Pf4-cre*; *Tgfb1*$^{flox/flox}$ and *Pf4-cre*; *Fgfr1*$^{flox/flox}$ mice[36–38], respectively. All experimental mice were a mix of male and female 8- to 12-week-old mice, except *Pf4-cre*; *Tgfb1*$^{flox/flox}$ mice, which were analyzed at a younger age (4 weeks old) to avoid potential compensatory mechanisms. 5FU (Sigma-Aldrich) was injected once in the tail vein at 150 μg per g body weight. After 5FU injection, mice were analyzed as described in the text. As indicated, recombinant TGF-β1 (PeproTech) at a dose of 40 μg per kg body weight or FGF1 (PeproTech) at a dose of 200 μg per kg body weight was injected intraperitoneally into mice following DT injection on the same day. All mouse strains used in this study had a C57BL/6J genetic background. Animals were randomly included in the experiments according to genotyping results. Animal experiments were conducted in a blinded fashion with respect to the investigator. The numbers of animals used per experiment are stated in the figure legends. All mice used in this study were housed in the animal facility at the Stowers Institute for Medical Research (SIMR) and were handled according to SIMR and US National Institutes of Health (NIH) guidelines. All procedures were approved by the Institutional Animal Care and Use Committee (IACUC) of the SIMR.

Flow cytometry. For phenotype analysis, hematopoietic cells were harvested from bone marrow (femur and tibia). Red blood cells were lysed using a 0.16 M ammonium chloride solution. For cell surface phenotyping, a lineage cocktail (Lin, phycoerythrin (PE)-Cy5) was used, including anti-CD3 (145-2C11), anti-CD4 (RM4-5), anti-CD8 (53-6.7), anti-Mac-1 (M1/70), anti-Gr1 (RB6-8C5), anti-B220 (RA3-6B2), anti-IgM (II/41) and anti-TER119 (TER-119) (100 ng antibody cocktail per million bone marrow cells, eBioscience). Monoclonal antibodies to SCA1 (D7, eBioscience), c-KIT (2B8, eBioscience), FLK2 (A2F10, eBioscience), CD34 (RAM34, eBioscience), CD48 (HM48-1, eBioscience), CD41 (MWReg30, eBioscience), CD42 (1C2, eBioscience), CD150 (TC15-12F12.2, BioLegend) and CD105 (MJ7/18, BioLegend) (all used as 50 ng per million bone marrow cells) were also used where indicated. For lineage analysis of peripheral blood, monoclonal antibodies to CD45.1 (A20, eBioscience), CD45.2 (104, eBioscience), CD3, B220, Mac-1 and Gr1 were used. 7-aminoactinomycin D (7-AAD) (A1310, Life technologies) was used to exclude dead cells. Cell sorting and analysis were performed using MoFlo (Dako), InFlux Cell Sorter (BD Biosciences), MACSQuant (Miltenyi Biotec) or CyAn ADP (Dako) instruments. Data analysis was performed using FlowJo software.

HSC culture and DT treatment. HSC expansion medium consisted of StemSpan serum-free expansion medium (SFEM) (Stem Cell Technologies) supplemented with 10 μg ml^{-1} heparin (Sigma), 0.5× penicillin-streptomycin (Sigma), 10 ng ml^{-1} recombinant mouse (rm) SCF (Biovision) and 20 ng ml^{-1} rmTHPO (Cell Sciences). Bone marrow cells harvested from *Pf4-cre*; *iDTR* mice were cultured with or without 50 ng ml^{-1} DT or 100 ng ml^{-1} FGF1 (PeproTech). HSC (CD34^{-}FLK2^{-}LSK cells) numbers were analyzed after 2 weeks of culturing.

Cell cycle analysis. Cell cycle analysis of HSCs was conducted with the BD Pharmingen PE Mouse Anti-Human Ki67 Set according to the manufacturer's instructions. The cells were further incubated with 0.1 μg μl^{-1} DAPI for 30 min at room temperature, followed by flow cytometric analysis with an InFlux Cell Sorter (BD Biosciences).

Transplantation. 2.0 × 10^5 CD45.2 bone marrow cells and 2.0 × 10^5 CD45.1 rescue bone marrow cells were transplanted into lethally irradiated (10 Gy) CD45.1 recipients. 2.0 × 10^4 bone marrow cells from *Pf4-cre*; *iDTR* mice (CD45.2) were cultured with DT and FGF1 as indicated for 2 weeks, and the culture products together with 2.0 × 10^5 CD45.1 rescue bone marrow cells were transplanted into lethally irradiated (10 Gy) CD45.1 recipients. 100 sorted LSK cells were cocultured with or without td-tomato–positive MKs from *Pf4-cre*; *R26R*^{tdT} (CD45.2) mice and transplanted together with 2.0 × 10^5 CD45.1 rescue bone marrow cells into lethally irradiated (10 Gy) CD45.1 recipients.

Repopulation assay. Every 4 weeks after transplantation, peripheral blood was collected from the submandibular vein. Hematopoietic repopulation was measured from donor-derived blood cells (CD45.2).

Immunostaining. Paraffin sections of bone were deparaffinized at 60 °C for 20 min. Sections were then treated with 100% xylene for 5 min twice, 100% ethanol for 5 min, 95% ethanol for 5 min and 70% ethanol for 5 min and rinsed with water for 1 min, followed by antigen retrieval with citrate buffer at 90 °C for 10 min. Blocking was done with Universal Blocking Reagent (BioGenex). Anti-vWF (rabbit, 1:100, ab75234, Abcam), anti-pSMAD2/3 (rabbit, 1:100, EMD Millipore) and anti-FABP4 (goat, 1:100, R&D Systems, AF1443) antibodies were used. Frozen sections were fixed using dry ice ethanol or 4% paraformaldehyde (PFA). Anti–TGF-β1 (LAP) (goat, 1:100, AB-246-NA, R&D System) and anti-vWF antibodies were used. Secondary staining was done with donkey anti-rabbit AF546 (1:200, Invitrogen) and donkey anti-goat AF488 (1:200, Invitrogen). Cell distances (HSCs to MKs and MKs to blood vessels) were measured and quantified using the Axiovision program (Zeiss). For HSC staining in bone sections, we used CD150-PE, CD48-allophycocyanin (APC), CD41-APC and Lin (B220, CD3, CD4, CD8, Gr1, IgM, Mac-1 and Ter119)-APC. For high-resolution three-dimensional images, *z*-stack collected images from LSM-510-VIS or LSM-710 confocal microscopy (Zeiss) were analyzed with Imaris software (Bitplane) and ImageJ.

RNA sequencing. The RNA sequencing library was prepared from approximately 200 ng RNA using the Illumina TruSeq RNA Sample Prep Kit (catalog number FC-122-1001), and sequencing was done using an Illumina HiSeq 2000. Libraries were prepared from CD31-GFP^{+} (VEGFR2^{+}CD45^{-}Ter119^{-}) cells, Nestin-GFP^{+} (CD45^{-}CD31^{-}Ter119^{-}) cells, SDF-1–RFP^{+} (CD45^{-}CD31^{-}Ter119^{-}) cells and mature Col2.3-GFP^{+} (CD45^{-}CD31^{-}Ter119^{-}) osteoblasts as described previously[39].

ELISA. For FGF1 and FGF2 detection, a monoclonal antibody to FGF1 (2 μg ml^{-1}, 500-P17, PeproTech) or FGF2 (2 μg ml^{-1}, BAM233, R&D Systems) was used for capture, and biotinylated antibodies to FGF1 (250 ng ml^{-1}, 500-P17Bt, PeproTech) or FGF2 (250 ng ml^{-1}, MAB233, R&D Systems) were used for detection using streptavidin–horseradish peroxidase (SA-HRP, 1 μg ml^{-1}, SNN2004, Invitrogen). Plates were read with an ELISA reader and analyzed according to the standard curve. The standard curve was made using rmFGF1 and rmFGF2 (PeproTech). TGF-β1 was measured using the Quantikine ELISA kit (R&D Systems) following the manufacturer's instructions.

TGF-β1 luciferase assay. We transiently transfected 293T cells with a TGF-β1–responsive luciferase promoter (CAGA-luc) (provided by H.Y. Lin, Massachusetts General Hospital) and a control *Renilla* luciferase (pRL-SV40) (Promega) vector with Lipofectamine (Invitrogen). Twenty-four hours after transfection, cells were serum starved in 1% FBS Opti-MEM and then incubated for 16 h with bone marrow supernatant (harvested as bone marrow extracellular fluids in PBS) from MK-ablated or control mice. As negative and positive controls, cells were incubated with either PBS or 5 ng ml^{-1} TGF-β1 (PeproTech). Experiments were performed in triplicate. We measured luciferase reporter activity with the Dual Reporter Assay (Promega) and determined relative luciferase activity as the ratio of luciferase units to *Renilla* units as described[40].

CFU-MK assays. MK progenitor assays were performed on bone marrow cells using MegaCult-C medium (Stem Cell Technologies) supplemented with 50 ng ml^{-1} rmTHPO, 20 ng ml^{-1} rmIL-6 and 10 ng ml^{-1} rmIL-3. CFU-MKs were stained for acetylcholinesterase activity and scored after 7 d of incubation according to the manufacturer's protocol.

Statistics. Statistical analyses were done using Student's *t* test. The results are shown as the mean ± s.e.m.

36. Xu, X., Qiao, W., Li, C. & Deng, C.X. Generation of Fgfr1 conditional knockout mice. *Genesis* **32**, 85–86 (2002).
37. Azhar, M. *et al.* Generation of mice with a conditional allele for transforming growth factor β1 gene. *Genesis* **47**, 423–431 (2009).
38. Meyer, A. *et al.* Platelet TGF-β1 contributions to plasma TGF-β1, cardiac fibrosis, and systolic dysfunction in a mouse model of pressure overload. *Blood* **119**, 1064–1074 (2012).
39. Sugimura, R. *et al.* Noncanonical Wnt signaling maintains hematopoietic stem cells in the niche. *Cell* **150**, 351–365 (2012).
40. Krause, D.S. *et al.* Differential regulation of myeloid leukemias by the bone marrow microenvironment. *Nat. Med.* **19**, 1513–1517 (2013).

doi:10.1038/nm.3706